

FAST TRACK COMMUNICATION

Adaptive resolution simulation of liquid water

Matej Praprotnik^{1,3}, Silvina Matysiak², Luigi Delle Site¹, Kurt Kremer¹
and Cecilia Clementi²

¹ Max-Planck-Institut für Polymerforschung, Ackermannweg 10, D-55128 Mainz, Germany

² Department of Chemistry, Rice University, 6100 Main Street, Houston, TX 77005, USA

E-mail: dellsite@mpip-mainz.mpg.de, kremer@mpip-mainz.mpg.de and cecilia@rice.edu

Received 8 June 2007, in final form 10 June 2007

Published 5 July 2007

Online at stacks.iop.org/JPhysCM/19/292201

Abstract

Water plays a central role in biological systems and processes, and is equally relevant in a large range of industrial and technological applications. Being the most important natural solvent, its presence uniquely influences biological function as well as technical processes. Because of their importance, aqueous solutions are among the most experimentally and theoretically studied systems. However, many questions still remain open. Both experiments and theoretical models are usually restricted to specific cases. In particular all-atom simulations of biomolecules and materials in water are computationally very expensive and often not possible, mainly due to the computational effort to obtain water–water interactions in regions not relevant for the problem under consideration. In this paper we present a coarse-grained model that can reproduce the behaviour of liquid water at a standard temperature and pressure remarkably well. The model is then used in a multiscale simulation of liquid water, where a spatially adaptive molecular resolution procedure allows one to change from a coarse-grained to an all-atom representation on-the-fly. We show that this approach leads to the correct description of essential thermodynamic and structural properties of liquid water. Our adaptive multiscale scheme allows for significantly greater extensive simulations than existing approaches by taking explicit water into account only in the regions where the atomistic details are physically relevant.

 Supplementary data are available from stacks.iop.org/JPhysCM/19/292201

1. Introduction

Scientific problems in physics are usually classified by typical scales of observable quantities such as energy, length or time. The appropriately determined scale together with a tailored model and/or experiment is the starting point of a successful study. The specific properties

³ On leave from: National Institute of Chemistry, Hajdrihova 19, SI-1001 Ljubljana, Slovenia.

under investigation then typically define the appropriate level of resolution. Using the optimal set of degrees of freedom (DOFs) guarantees efficiency, accuracy and avoids huge amounts of unnecessary detail, which might even obscure the underlying physics. This approach dates back to the very beginning of modern physics and finds its logical continuation in systematic coarse-graining efforts for modern computational materials science and biophysics problems [1–4], where full-blown all-atom simulations are often beyond the possibilities of current and near-future computers. However, in many problems in materials science and biology different time and length scales are intrinsically interconnected, far beyond giving constant prefactors at the next coarser level of detail. Multiscale simulations are emerging as a promising tool for such problems [5–14]. Ideally, in addition to coarse-graining one would like to be able to step back to characteristic fine-grained configurations as well [15, 16]. Recently, an adaptive multiscale scheme (AdResS) has been proposed by some of us that also allows a free exchange of particles between regions of different resolution and to adjust locally the level of detail at will, while maintaining equilibrium with the fluctuating environment [17].

In this paper we address the above issue for liquid water, which continues to be a very active research field, for the obvious reason that water is the biological solvent of choice. Although many classical models have been developed for the simulation of liquid water [18–21], there is still no unique model that can reproduce all of its anomalous properties. Water, though a small molecule, intrinsically influences its surroundings on multiple scales and plays different roles at different scales. For instance, in the case of biomolecules in solution, at short length scales the hydrogen bonding with water governs the local shape and stability of folded biopolymers, whereas the ‘hydrophobic effect’ drives the organization of the system at longer time and length scales (for instance in the formation of membranes in aqueous solution). The approach presented in this paper represents a first step towards multiscale modelling of such complex scenarios. For fluctuating systems, such as adsorption of water on a hydrophilic surface, we envisage a system in which an atomistic description is needed only near the surface, and a mesoscopic resolution can be used for water molecules further away, with molecules freely moving around and interacting with each other only with the local, more or less detailed level of resolution. Another typical example where our method will find application is that of a solvated macromolecule, e.g. a protein in water. In such a system, the solvent surrounding the macromolecule can be represented with a sufficiently high level of detail so that the specific interactions between the solvent and the solute will be correctly taken into account. On the other hand, the solvent farther away from the macromolecule, where the high resolution is not needed, can be represented on a coarse-grained level [22].

To accomplish this goal, we first propose and test a new single-site water model that reproduces the essential thermodynamic and structural features remarkably well, e.g. the tetrahedral packing of liquid water at standard external conditions, as obtained by detailed all-atom simulations⁴. The definition of this new single-site coarse-grained water model is needed for an adaptive resolution simulation, in order to match to the original all-atom model sufficiently well to have a smooth and fast transition between resolutions. Previously proposed simplified water models do not have the required properties to obtain such a smooth transition.

In the second step we adapt the AdResS scheme to define a robust and physically accurate procedure to smoothly join the explicit regions of atomistic and coarse-grained resolution. The resulting multiscale hybrid/mesoscopic model system [17, 23–25] is composed of explicit and coarse-grained molecules as presented in figure 1.

⁴ The coarse-grained model, as it is presented here, has been designed to perform well specifically for the selected temperature and pressure (standard external conditions). However, one can adjust the model for different thermodynamic conditions by a re-parametrization of the effective potential between molecules.

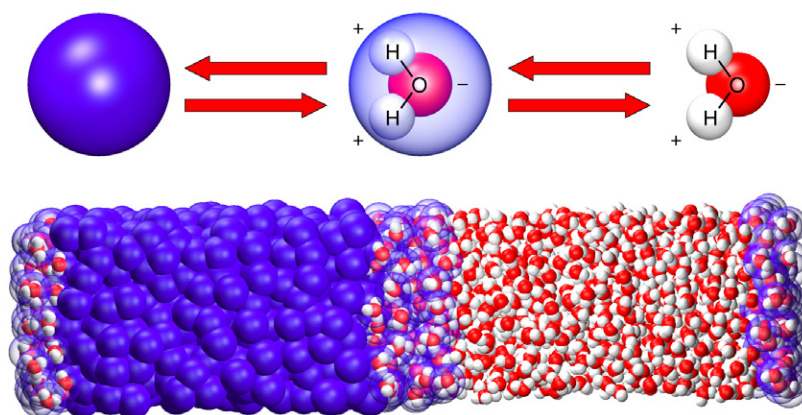


Figure 1. On-the-fly interchange between the all-atom and coarse-grained water models. Top: the explicit all-atom water molecule is represented at the right, and the coarse-grained molecule at the left. The middle hybrid molecule interpolates between the two (see text). Bottom: a schematic representation of the full system, where a hybrid region connects the explicit and coarse-grained levels of description. All the results presented in the paper were obtained by performing NVT simulations using ESPResSo [26] with a Langevin thermostat, with a friction constant $\Gamma = 5 \text{ ps}^{-1}$ and a time step of 0.002 ps at $T_{\text{ref}} = 300 \text{ K}$ and $\rho = 0.96 \text{ g cm}^{-3}$ (the density was obtained from an NPT simulation with $P_{\text{ref}} = 1 \text{ atm}$). Periodic boundary conditions were applied in all directions. The box size is 94.5 Å in the x direction and 22 Å in the y and z directions. The width of the interface layer is 18.9 Å in the x direction.

2. Coarse-graining of water

Recent work has focused on simplified coarse-grained models that can reproduce qualitatively the all-atom centre-of-mass radial distribution function (rdf) of water [27–31]. To reproduce further structural properties, such as the orientational preferences for nearest neighbour configurations (that is essential for hydrogen bonding), previous one-site models [28, 29] require *a posteriori* adjustment of the local environment [29]. The one-site model of water presented in this paper can reproduce the structural and thermodynamic properties of a widely used all-atom water model (namely, Rigid TIP3P [18]) at standard temperature and pressure with remarkable accuracy, without requiring any orientational corrections⁵. To construct the model we follow an iterative inverse statistical mechanics approach proposed by Lyubarstev *et al* [32] (for alternative procedures see also [2] and [33]). The aim of this scheme is to numerically build a coarse-grained effective Hamiltonian that can mimic the behaviour of a set of physical observables (in this case the centre-of-mass rdf) of the system under consideration (see, e.g., Matysiak *et al* [34, 35] where this idea has been used to define a coarse-grained protein Hamiltonian ‘anchored’ to experimental data). Additionally, in order to match the pressure of the coarse-grained to the all-atom model, after each iteration, a weak constant force is added to the effective force in such a way that the total effective force and potential energy are zero at the 7 Å cut-off distance [23, 33].

Figure 2 shows the final results obtained when this procedure is applied to a box of water molecules (see section 4 for details). Perfect agreement between the all-atom and coarse-grained centre-of-mass rdfs is reached with our optimized effective potential (shown in the inset

⁵ Since a water molecule is electrically neutral the interaction site has a zero electric charge. Furthermore, in contrast to a Stockmayer fluid, the presented one-site model does not have a dipole (or any higher electric multipole). All the electrostatic interactions, including the reaction field correction, are therefore implicitly taken into account via the effective intermolecular potential.

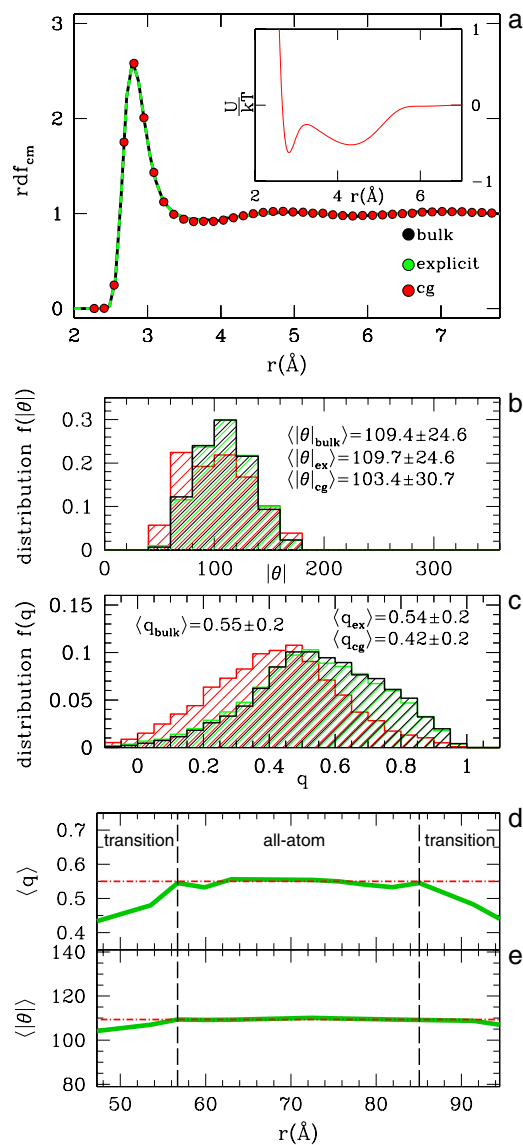


Figure 2. (a) The centre-of-mass rdfs for explicit (ex) (green line) and coarse-grained (cg) (red line) regions of the hybrid system, are shown together with the rdfs corresponding to a bulk all-atom simulation (black line). The local O–H and H–H rdfs for the explicit molecules in the hybrid system compare equally well to the standard bulk simulations (not shown). The optimized effective potential for the coarse-grained model is shown in the inset as a function of inter-particle separation, r . (b) The distribution of the angle θ formed between the centres-of-mass of three nearest neighbours for the three cases studied as given in (a). (c) The analogous distributions of the orientational order parameter q . (d) Average orientational order parameter q as a function of the coordinate x in the simulation box. (e) Average centre-of-mass angular distribution between three nearest neighbours as a function of the coordinate x in the simulation box.

of the figure) after eight iterations. The tabulated values of the potential used in the simulations are provided in the supplementary material (available at stacks.iop.org/JPhysCM/19/292201).

The effective potential has a first primary minimum at about 2.8 Å corresponding to the first peak in the centre-of-mass rdf. The slightly weaker and significantly broader minimum at 4.5 Å corresponds to the second hydration shell. The combined effect of the two minima leads to a local packing close to that of the all-atom TIP3P water. The average number of nearest neighbours (as obtained by integrating the rdf over the first hydration shell) is 3.92 ± 0.28 in the explicit region, and 4.14 ± 0.33 in the coarse-grained region, in both cases signalling a tetrahedral packing⁶. Our effective coarse-grained potential is qualitatively different from the previously suggested potentials [27–29]: while in previous one-site models the deepest minimum corresponds to the second hydration shell, the absolute minimum in our model is found in the first shell. In order to more thoroughly quantify the structural properties of our model, which are not completely defined by the rdf, we computed the angular distribution between the centre-of-masses of three nearest neighbour molecules and the distribution of the orientational order parameter q as defined by Errington *et al* [37]: $q = 1 - \frac{3}{8} \sum_{j=1}^3 \sum_{k=j+1}^4 (\cos \psi_{jk} + \frac{1}{3})^2$, where ψ_{jk} is the angle formed by the lines joining the oxygen atom of a given molecule (the centres of the spheres in the one-site coarse-grained model, respectively) and those of its nearest neighbours j and k . The parameter q measures the extent to which a molecule and its four nearest neighbours adopt a tetrahedral arrangement [37]. The good agreement between the explicit and coarse-grained water models shown in figures 2(b) and (c) indicates that although our coarse-grained model is spherically symmetric and does not have any explicit directionality, it approximately captures the orientational preferences of hydrogen bonding.

It is worth noting that the coarse-graining significantly speeds up the simulation, with a total gain in computational time of a factor ~ 17 – 20 when compared to atomistic simulations. Two factors contribute to this speed-up:

- (i) The reduction on the number of interactions computed at each time step and the simplified form of interactions associated with the coarse-graining accounts for a factor ~ 8 – 10 .
- (ii) In addition, there is an intrinsic timescale difference in the diffusive dynamics of the coarse-grained system, which is faster by about a factor of 2 than the predictions of all-atom simulations because of the reduced number of DOFs (the diffusion coefficient of the centre-of-mass for the Rigid TIP3P model is $D \approx (3.7 \pm 0.3) \times 10^{-9} \text{ m}^2 \text{ s}^{-1}$ while for the coarse-grained model it is $D \approx (8.1 \pm 0.4) \times 10^{-9} \text{ m}^2 \text{ s}^{-1}$).

While an accelerated timescale can be very advantageous in many applications, if required, the same diffusion timescale as in the atomistic model can be restored in the coarse-graining by adjusting D with an increased background friction in the Langevin thermostat [2, 38].

3. Multiscale water

In order to smoothly couple the atomistic and coarse-grained resolutions, we adapt the multiscale AdResS (adaptive resolution scheme) procedure of Praprotnik *et al* [17, 23] outlined in section 4 to directly link a model system composed of explicit and coarse-grained molecules. Detailed comparisons between the bulk explicit simulations and the explicit regime in our hybrid set-up prove that our approach does not alter the structural properties of the water model studied.

⁶ Our single-site model is therefore significantly different from a Lennard-Jones liquid, which is closely packed with 12 nearest neighbours (see for instance [36]). Indeed, results from extensive tests show that if the functional form of a Lennard-Jones potential is used in the definition of the water coarse-grained model, the iterative inverse statistical mechanics procedure does not converge, and the rdf of the explicit model cannot be reproduced (results not shown).

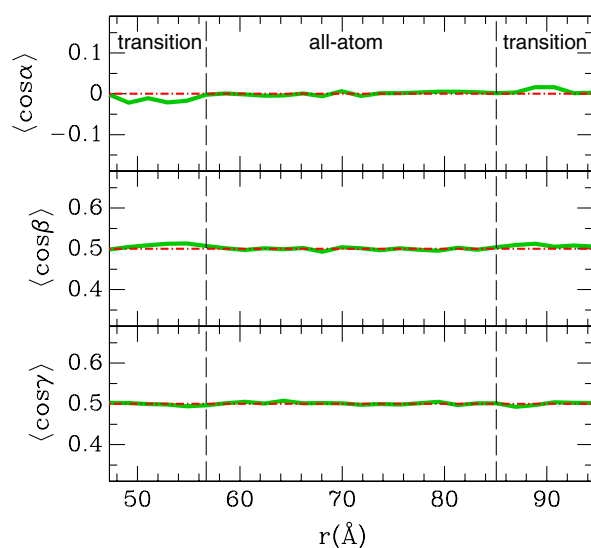


Figure 3. Average cosine value of the angle formed by the dipole vector (top panel), the vector joining the two hydrogen atoms of a molecule (middle panel) and the vector normal to the plane of a molecule (bottom panel) with the interface normal vector pointing toward the coarse-grained region as a function of the coordinate x in the simulation box. The results demonstrate that the water molecules have a random orientation both in the explicit and transition regimes. The transition regime thus neutralizes the possible orientational effect of the coarse-grained regime so that the water in the explicit regime has the same structural properties as the all-atom bulk water.

When explicit water molecules approach a neutral fluid surface (as happens upon entering the coarse-grained liquid water region) the hydrogen bond network formed among the explicit molecules can be strongly perturbed. As a result, the explicit molecules near the resolution interface could orient and behave differently from the bulk. However, this spurious effect can be avoided by using an appropriate interface layer between the explicit and coarse-grained regime. It has been shown that the perturbation introduced by the interaction of explicit water with a neutral surface extends around 10 \AA into the water layer [39]. This distance is comparable to the maximum range of electrostatic interactions in our simulations. This distance range determines the width of the interface layer to allow the molecules to equilibrate on-the-fly while moving from one resolution to the other. The results presented in this paper have been obtained by using a conservative choice for the width of the interface layer, that is, double the maximum range of interactions⁷.

The results presented in figure 3 show that indeed the interface layer completely removes any orientational bias that could have been introduced in the explicit water by the interactions with the coarse-grained regime. The average orientations of three vectors are shown in the figure, namely the dipole moment of a water molecule, the vector perpendicular to the plane of the molecule and the vector joining the two hydrogen atoms of the molecule, as a function of the coordinate x spanning across the two resolutions in the simulation box. We denote the angles formed by these vectors and the normal vector pointing towards our coarse-grained water liquid as α , β and γ , respectively. The average orientation of the vectors can be quantified by

⁷ However, a smaller interface layer can be used without affecting the fluxes between the layers or the results in the two resolution regimes (results not shown).

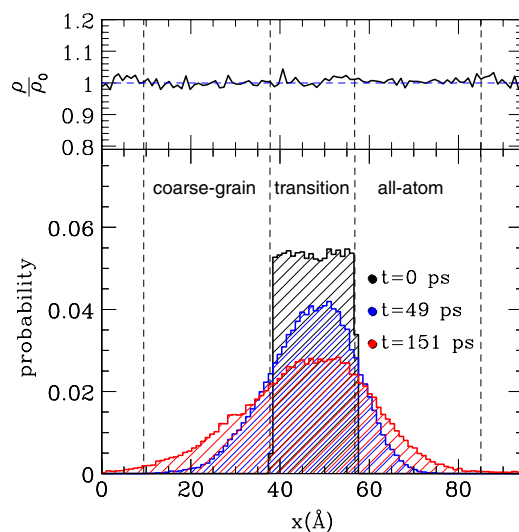


Figure 4. Top figure: normalized density profile in the x direction of the hybrid system. Bottom figure: time evolution of a diffusion profile for the molecules that are initially (at time $t = 0$ ps) located in the interface region. The diffusion profile is averaged over ≈ 400 different time origins. Vertical lines denote the boundaries of the interface layer.

the average cosine value of these angles⁸. The results in figures 2(d), (e), and 3 indicate that the transition regime neutralizes the interface effect of the coarse-grained liquid water, such that the molecules have fully equilibrated orientational DOFs when they enter the explicit regime.

The structural (see figure 2) and thermodynamic properties of the bulk all-atom simulations are correctly reproduced by the hybrid system with the same mean temperature (0.1% difference) and pressure (0.5% difference). The normalized density for the hybrid system is homogeneous in the coarse-grained and explicit regions with (very) small oscillations in the transition regime (see figure 4). In order to prove the free exchange of molecules between the different regimes we have computed the time evolution of a diffusion profile for molecules that were initially localized at the interface layer. Figure 4 shows that these molecules spread out asymmetrically with time. This asymmetry arises from the aforementioned difference in diffusion coefficient between the all-atom and coarse-grained regions. It is possible to obtain the same diffusional dynamics across the different resolutions by adding a local Langevin thermostat, as mentioned above (unpublished results). However, it is worth stressing that this difference in timescale can be advantageous for reaching longer simulation times in systems where multiple length- and time scales are intrinsically present.

4. Model and methods

In the present study, half of the simulation box is occupied by atomistic (Rigid TIP3P) water molecules while the other half is filled with the same number of corresponding coarse-grained molecules as schematically presented in figure 1. The two regions freely exchange molecules

⁸ The random orientation corresponds to $\langle \cos \beta \rangle = \langle \cos \gamma \rangle = 0.5$ for the molecular normal vector, and for the vector joining the two hydrogens, while the random orientation of the dipole moment corresponds to $\langle \cos \alpha \rangle = 0$. The different values for the random orientations of the vectors arise from the fact that opposite directions are physically indistinguishable both for the molecular normal vector and the vector joining the two hydrogens, while the vector of the dipole moment has a specific directionality [39].

through a transition regime, where the molecules change their resolution and their number of DOFs accordingly. The interface region contains hybrid molecules that are composed of an all-atom molecule with an additional massless centre-of-mass particle serving as an interaction site. The transition, which needs to be smooth in order to be used in molecular dynamics simulations, is governed by a weighting function $w(x) \in [0, 1]$ that interpolates the interaction forces between the two regimes, and assigns the identity of the particle. We used the weighting function defined in [17] in such a way that $w = 1$ corresponds to the atomistic region, and $w = 0$ to the coarse-grained region, whereas the values $0 < w < 1$ correspond to the interface layer. The atomic and mesoscopic length scales are coupled via the intermolecular force acting between centres-of-mass of molecule α and β as:

$$\mathbf{F}_{\alpha\beta} = w(X_\alpha)w(X_\beta)\mathbf{F}_{\alpha\beta}^{\text{atom}} + [1 - w(X_\alpha)w(X_\beta)]\mathbf{F}_{\alpha\beta}^{\text{cm}}, \quad (1)$$

where $\mathbf{F}_{\alpha\beta}^{\text{atom}} = \sum_{i_\alpha, j_\beta} \mathbf{F}_{i_\alpha j_\beta}^{\text{atom}} = -\sum_{i_\alpha, j_\beta} \frac{\partial U^{\text{atom}}}{\partial \mathbf{r}_{i_\alpha j_\beta}}$ is the sum of all pair intermolecular atom interactions between explicit atoms of the molecules α and β and $\mathbf{F}_{\alpha\beta}^{\text{cm}} = -\frac{\partial U^{\text{cm}}}{\partial \mathbf{R}_{\alpha\beta}}$ is the corresponding effective intermolecular force between their centres-of-mass. $\mathbf{r}_{i_\alpha j_\beta} = \mathbf{r}_{i_\alpha} - \mathbf{r}_{j_\beta}$ is the vector between atom i in molecule α and atom j in molecule β and $\mathbf{R}_{\alpha\beta} = \mathbf{R}_\alpha - \mathbf{R}_\beta$ the vector between the centres-of-mass of molecules α and β , with the corresponding X coordinates X_α and X_β . Each time a molecule crosses a boundary between the different regimes it gains or loses (depending on whether it leaves or enters the coarse-grained region) its equilibrated rotational DOFs while retaining its linear momentum. To supply or remove the latent heat caused by the switch of resolution this method is employed together with a Langevin thermostat [17]. In order to remove an increased pressure in the transition regime, an interface pressure correction, as tested in [23], is employed. As discussed in an earlier publication, it is important to interpolate the forces and not the interaction potential if Newton's third law is to be satisfied [24]. The key methodological issue in applying our approach to water is how to treat the long-range electrostatic interactions. We have chosen the reaction field (RF) method, in which all molecules outside a spherical cavity of a molecular-based cut-off radius $R_c = 9 \text{ \AA}$ are treated as a dielectric continuum with a dielectric constant ϵ_{RF} [42–45]. The Coulomb force acting on a partial charge e_{i_α} , belonging to the explicit or hybrid molecule α , at the centre of the cut-off sphere, due to a partial charge e_{j_β} , belonging to the explicit or hybrid molecule β , within the cavity is:

$$\mathbf{F}_{C_{i_\alpha j_\beta}}^{\text{atom}}(\mathbf{r}_{i_\alpha j_\beta}) = \frac{e_{i_\alpha} e_{j_\beta}}{4\pi\epsilon_0} \left[\frac{1}{r_{i_\alpha j_\beta}^3} - \frac{1}{R_c^3} \frac{2(\epsilon_{\text{RF}} - 1)}{1 + 2\epsilon_{\text{RF}}} \right] \mathbf{r}_{i_\alpha j_\beta}. \quad (2)$$

There are three main reasons that make the RF method a natural choice to be applied with our scheme (equation (1)): the first reason is that it does not impose any artificial periodicity (that would interfere with the definition of the interface layer of the system), the second one is the pairwise form of the reaction field term (equation (2)), and the third one is that, as in our scheme, the RF method works accurately only in a combination with a thermostat [45]. The last point can be better understood if the switching of the resolution is seen in analogy to a geometry-induced phase transition [24].

5. Conclusion

We have presented a general and computationally efficient multiscale model for water. We have shown that a new one-site coarse-grained model for water molecules can reproduce thermodynamic and structural properties of the Rigid TIP3P water model remarkably well, and that a smooth transition and free exchange between coarse-grained and all-atom resolutions

is possible. The presented multiscale approach can be applied to any other either flexible or rigid non-polarizable classical water model, e.g. SPC or SPC/E [40–42]. We envisage that such a multiscale resolution of water will play an important role in the modelling of wet/dry interfaces and in biomolecular simulations. The gain in computational speed will allow for larger systems and more systematic studies and should at the same time extend the possibilities of such simulations to a larger user group.

Acknowledgments

We wish to thank the NSF-funded Institute for Pure and Applied Mathematics at UCLA where this work was first planned. This work has been supported in part by grants from NSF(CAREER CHE-0349303, CNS-045433 and CCF-0523908), Texas-ATP (003604-0010-2003), the Robert A Welch Foundation (Norman-Hackerman Young Investigator award and C-1570) (CC) and the Volkswagen Foundation (KK & LDS). The Rice University Cray XD1 Cluster ADA used for the calculations is supported by the NSF under grant CNS-0421109, and a partnership between Rice University, AMD and Cray.

References

- [1] Nielsen S O, Lopez C F, Srinivas G and Klein M L 2004 *J. Phys.: Condens. Matter* **16** R481
- [2] Izvekov S and Voth G A 2006 *J. Chem. Phys.* **125** 151101
- [3] Harmandaris V A, Adhikari N P, Van der Vegt N F A and Kremer K 2006 *Macromolecules* **39** 6708
- [4] Das P, Matysiak S and Clementi C 2005 *Proc. Natl Acad. Sci. USA* **102** 10141
- [5] Delle Site L, Abrams C F, Alavi A and Kremer K 2002 *Phys. Rev. Lett.* **89** 156103
- [6] Neri M, Anselmi C, Cascella M, Maritan A and Carloni P 2005 *Phys. Rev. Lett.* **95** 218102
- [7] Koumoutsakos P 2005 *Annu. Rev. Fluid Mech.* **37** 457
- [8] Backer J A, Lowe C P, Hoefsloot H C J and Ledema P D 2005 *J. Chem. Phys.* **123** 114905
- [9] Fabritiis G D, Delgado-Buscalioni R and Coveney P V 2006 *Phys. Rev. Lett.* **97** 134501
- [10] Lyman E, Ytreberg F M and Zuckerman D M 2006 *Phys. Rev. Lett.* **96** 028105
- [11] Shi Q, Izvekov S and Voth G A 2006 *J. Phys. Chem. B* **110** 15045
- [12] Christen M and van Gunsteren W F 2006 *J. Chem. Phys.* **124** 154106
- [13] Weinan E, Engquist B, Li X, Ren W and Vanden-Eijnden E 2007 *Commun. Comput. Phys.* **2** 367
- [14] Shehu A, Clementi C and Kavraki L 2006 *Proteins Struct. Funct. Bioinf.* **65** 164
- [15] Heath A, Kavraki L and Clementi C 2007 *Proteins Struct. Funct. Bioinf.* **68**
- [16] Hess B, Leon S, Van der Vegt N and Kremer K 2006 *Soft Matter* **2** 409
- [17] Praprotnik M, Delle Site L and Kremer K 2005 *J. Chem. Phys.* **123** 224106
- [18] Jorgensen W L, Chandrasekhar J, Madura J D, Impey R W and Klein M L 1983 *J. Chem. Phys.* **79** 926
- [19] Mahoney M W and Jorgensen W L 2000 *J. Chem. Phys.* **112** 8910
- [20] Praprotnik M and Janežič D 2005 *J. Chem. Phys.* **122** 174103
- [21] Guillot B 2002 *J. Mol. Liq.* **101** 219
- [22] Praprotnik M, Delle Site L and Kremer K 2007 *J. Chem. Phys.* **126** 134902
- [23] Praprotnik M, Delle Site L and Kremer K 2006 *Phys. Rev. E* **73** 066701
- [24] Praprotnik M, Kremer K and Delle Site L 2007 *Phys. Rev. E* **75** 017701
- [25] Praprotnik M, Kremer K and Delle Site L 2007 *J. Phys. A: Math. Theor.* **40** F281
- [26] Limbach H J, Arnold A, Mann B A and Holm C 2006 *Comput. Phys. Commun.* **174** 704
- [27] Garde S and Ashbaugh H S 2001 *J. Chem. Phys.* **115** 977
- [28] Voth G A and Izvekov S 2005 *J. Chem. Phys.* **123** 134105
- [29] Head-Gordon T and Stillinger F H 1993 *J. Chem. Phys.* **98** 3313
- [30] Soper A K 1996 *Chem. Phys.* **202** 295
- [31] Nezbeda I 2005 *Mol. Phys.* **103** 59
- [32] Lyubartsev A P and Laaksonen A 1995 *Phys. Rev. E* **52** 3730
- [33] Reith D, Putz M and Müller-Plathe F 2003 *J. Comput. Chem.* **24** 1624
- [34] Matysiak S and Clementi C 2004 *J. Mol. Biol.* **343** 235
- [35] Matysiak S and Clementi C 2006 *J. Mol. Biol.* **363** 297

- [36] Lazaridis T and Karplus M 1996 *J. Chem. Phys.* **105** 4294
- [37] Errington J R and Debenedetti P G 2001 *Nature* **409** 318
- [38] Kremer K and Grest G S 1990 *J. Chem. Phys.* **92** 5057
- [39] Jedlovszky P, Vincze A and Horvai G 2004 *Phys. Chem. Chem. Phys.* **6** 1874
- [40] Berendsen H J C, Postma J P M, van Gunsteren W F and Hermans J 1981 *Intermolecular Forces* ed B Pullman (Dordrecht: Reidel) p 331
- [41] Berendsen H J C, Grigera J R and Straatsma T P 1987 *J. Phys. Chem.* **91** 6269
- [42] Praprotnik M, Janežič D and Mavri J 2004 *J. Phys. Chem. A* **108** 11056
- [43] Neumann M 1983 *Mol. Phys.* **50** 841
- [44] Neumann M 1985 *J. Chem. Phys.* **82** 5663
- [45] Tironi I G, Sperb R, Smith P E and van Gunsteren W F 1995 *J. Chem. Phys.* **102** 5451